Powder Technology 301 (2016) 421–428

Contents lists available at ScienceDirect

Powder Technology

journal homepage: www.elsevier.com/locate/powtec

Influence of milling parameters on particle size of ulexite material

Sezai Kutuk *

Department of Physics, Faculty of Science and Letters, Artvin Coruh University, 08100 Artvin, Turkey
Department of Electronics and Automation, Vocational School of Technical Sciences, Recep Tayyip Erdogan University, 53100 Rize, Turkey

ARTICLE INFO

Article history:
Received 8 March 2016
Received in revised form 21 May 2016
Accepted 14 June 2016
Available online 16 June 2016

Keywords:
Ulexite
Mechanical milling
Particle size
Morphology
Crystalline size
Nano-sized

ABSTRACT

Commercial raw ulexite (U) materials were milled from 0 h to 8 h by using mechanical milling technique for various initial powder size (−3 mm; −75 μm), ball to powder ratio (5:1; 10:1), and ball size (10 mm; 5 mm). Particle size, morphology, elemental, and crystal structure measurements of the milled powders were performed. In the particle size distribution analysis, the smallest d_{50} and d_{10} values were respectively found as 8.846 μm and 790 nm for U_5m powder (obtained from that initial powder with −3 mm in size was milled by balls with 5 mm in size) at 0.5 h. In the morphology analysis, the microstructure of the U_5m powder was observed to be more homogeneous by means of milling process. In the elemental analysis, it was deduced that the U_5m powder is not a pure compound. In the crystal structure analysis, it was determined that the crystal structure of the U_5m powder is exponentially deteriorated with increasing the milling time, and then it has become an amorphous structure at the end of 8 h. The crystalline size of the U_5m powder is reduced to 15.5 nm after 4 h of milling. The results of this study are considered to be useful for future nano studies and industrial applications of ceramic ulexite compound, which is a boron mineral.

1. Introduction

Approximately 73% of boron reserves, containing 955 million tons of boron oxide (B_2O_3) known on the worldwide, exist in Turkey [1]. A large number of commercially recovered boron reserves consist of colemanite, ulexite, tincal and pandermite minerals (borates, which are an extraordinarily large group of minerals). Among these minerals, the ceramic ulexite compound has a chemical formula of $Na_2O{\cdot}2CaO{\cdot}5B_2O_3{\cdot}16H_2O$ (sodium-calcium-borate hydrate) and has found in large amounts in Turkey. The ulexite mineral has been usually obtained together with other borates. Demand for the ulexite mineral has rapidly increased up to now because of the fact that it is utilized as a raw material in the production of boron compounds. The ulexite mineral has extensive industrial applications such as fabrication of glass, porcelain, leather, cosmetics and photographic chemicals, detergent materials, polymer, catalysts, steel, refractory materials, fertilizers, disinfectant, food preservative, textiles, nuclear fiberglass, insulators, etc. [2,3]. Besides, it has potential technological applications such as hydrogen energy ($NaBH_4$) [4], superconducting material (MgB_2) [5], shielding material [6], ultra-high temperature ceramic material (ZrB_2) [7], cement concrete [8], asphalt concrete [9], brick [10]. Therefore, the ulexite mineral is an important mineral at both scientific and technological community owing to its attractive physical and mechanical properties.

Nano-sized materials have been intensely studied due to their better physical, mechanical and magnetic properties compared to micro-sized materials. This reason is in reduction of crystalline/particle size of the material to nano-scale level. In order to accomplish this, there are many preparation techniques. One of the beneficial techniques is mechanical milling (MM). The MM technique can easily provide the nano-sized powders with cheaper equipment, and thus it can be a great potential to be used for mass production [11]. This technique is a solid-state reaction process including repeated deformation, welding and fracturing of the powder particle. A lot of materials such as amorphous alloys, inter-metallic compounds, composites and ceramics have been prepared by using the MM technique. As a result of the MM technique, the final product powder has generally a nano-sized structure indicating better properties in comparison to micro-sized structure [12]. For example, nano-sized ceramic materials show better sinterability, strength, fracture toughness, resistance to oxidation and creep resistance [7].

The MM technique is performed by the high-energy ball milling. There are various types of ball milling techniques in relation to the motion of balls and vial(s) such as planetary, vibration and attritor. Among them, the planetary ball milling depends on different parameters affecting the particle size refinement. These parameters are milling time, ball to powder (weight) ratio (BPR), process control agent (PCA), size of the ball, size of the vial, rotation speed, atmosphere of milling, etc.

* Department of Physics, Faculty of Science and Letters, Artvin Coruh University, 08100 Artvin, Turkey.
E-mail addresses: sezai_kutuk@hotmail.com, sezai.kutuk@erdogan.edu.tr.

http://dx.doi.org/10.1016/j.powtec.2016.06.020
0032-5910/

Therefore, selection of the parameters is significant since it changes considerably with type of the material used [13,14].

Li et al. revealed that nano-particles of boron nitride (BN) were synthesized from B_2O_3 by a ball milling technique and annealing process. Firstly, average particle size of the B_2O_3 powder is reduced from 200 μm to 20 μm after 60 h of milling time. Eventually, the nano-particles generally disperses uniform and their diameters are in the range of 20–100 nm. In addition, most of them are close to 70 nm in diameter (average particle size) [15]. Jung et al. published that nano-sized BN powder was produced by a ball milling technique and its average grain/particle size decreases from 10 μm (initial size) to 100 nm (final size) [16].

Alizadeh et al. declared that nano-structured B_2O_3 powder was prepared by a ball milling technique and the crystalline size of the B_2O_3 powder is reduced from >100 nm to 19 nm after 5 h of milling time [11].

Xu et al. investigated that boron (B) powder was ground by using a ball milling technique and it was employed to fabricate a superconducting material (MgB_2). They determined to improve the critical current density (J_c) of the material with the crystalline size refinement of 100 nm [17]. Jung et al. reported that B powders with average initial particle size of 800 nm were ground by a ball milling technique under dry milling and wet milling processes. The smallest particle sizes are 58 nm and 220 nm under the dry and wet milling processes, respectively [18].

Zhang et al. examined that SiBCN powder largely comprises of near-spherical agglomerates 6.6 ± 5.3 μm in average particle size resulting from the hard agglomeration of nano-primary particles, which were fabricated by using a ball milling technique. However, they observed that in fact these nano-primary particles are 190.8 ± 33.6 nm in average particle size [19]. In another study, they found that SiBCN powder has an average particle size ranging from 4.6 μm to 5.3 μm due to agglomerate, but average particle size of nano-primary particles is 190.8 ± 33.6 nm. Furthermore, optimization parameter values of milling process were determined as 600 rpm in milling speed, 20:1 in BPR and 30–40 h in milling time [20].

Vignola et al. investigated that nano-structured B powder was achieved with average grain size of 80 nm. The B powder was used to synthesize a MgB_2 superconducting material and consequently increases its superconducting properties such as J_c and the critical temperature. Thus, it is indicated that the B powder works very well which makes it possible for a development on large scale fabrication [5].

No studies have been conducted yet considering optimum condition of nano-sized ulexite material by milling in terms of both science and applied engineering in the literature. Therefore, the main aim of this study is to examine the effect of milling parameters on the particle size of the ulexite material. Afterward, in another study, the best results obtained from here will be employed in both cement concrete and asphalt concrete at civil engineering for the purpose of investigating influence of the nano-sized ulexite material.

2. Experimental details

2.1. Materials

Commercial raw ulexite (U) materials in this study were supplied from Eti Mine Works General Management's Bigadic Boron Mine (Eti Maden) in Turkey. These materials which were eliminated −3 mm (coarse powder, U-3m) and −75 μm (fine powder, U-75μ) scaled sieves with the ASTM (the American Society for Testing and Materials) standard were used as initial materials. Chemical composition analyses of the initial materials were carried out by the Eti Maden, and their results are presented in Table 1 [21,22]. Composition difference between the U-3 m and the U-75 μ materials is attributed that the raw ulexite material mined passes through several physical and chemical processes (washing, crushing, sieving, decomposition, dissolution, milling and so on).

Table 1
Chemical composition analyses of ulexite initial materials.

Compound	Ulexite (wt.%)	
	−3 mm	−75 μm
B_2O_3	25.50 ± 1.50	37.00 ± 1.00
CaO	21.00 ± 3.00	19.00 max
SiO_2	13.00 max	4.00 max
Na_2O	2.00 min	3.50 max
SO_4	0.60 max	0.25 max
As	40 ppm max	40 ppm max
MgO		2.50 max
SrO		1.00 max
Al_2O_3		0.25 max
Fe_2O_3		0.04 max
Humidity		1.00 max

2.2. Milling process

The initial materials were ground by a planetary high-energy ball mill for 0.5 h, 1 h, 2 h, 4 h and 8 h, respectively. Mechanical milling process was performed by using this mill (Retsch, model 'PM 100') and using a 250 ml zirconium oxide vial and both 5 mm and 10 mm in diameter zirconium oxide balls at room temperature [23]. BPR and rotational speed was 10:1; 5:1 and 500 rpm, respectively. In order to prevent overheating during milling, the mill was stopped every 15 min and then resumed after 5 min in the opposite direction. Table 2 shows details of the milling experiments.

Milling names were henceforth respectively termed as U; U_75μ; U_10:1; U_5m for simplicity instead of that U_3m_5:1_10m; U_75μ_5:1_10m; U_3m_10:1_10m; U_3m_5:1_5m were written in following format: Powder name_Initial powder size_BPR_Ball size (see Table 3).

2.3. Measurements

The particle size distributions of the initial materials and milled powders were measured by a laser size analyzer (Malvern, model 'Mastersizer Hydro 2000 MU'). This analyzer scanned four times and then averaged for each powder. d_{50}, d_{10} and d_{min} values corresponding to respectively 50%, 10% and minimum percent passing volumes were determined from the particle size distribution.

Table 2
Milling parameters and their average particle sizes.

Experimental no.	Initial powder size (m)	BPR	Ball size (mm)	Milling time (h)	d_{50} (μm)
1	−3m	5:1	10	0	444.220
2				0.5	14.331
3				1	63.836
4				2	67.631
5				4	22.528
6				8	19.034
7	−75μ	5:1	10	0	11.524
8				0.5	21.453
9				1	18.585
10				2	15.679
11				4	13.964
12				8	18.526
13	−3m	10:1	10	0.5	22.282
14				1	25.757
15				2	18.732
16				4	12.087
17				8	10.582
18	−3m	5:1	5	0.5	8.846
19				1	13.786
20				2	14.979
21				4	17.994
22				8	14.242

Table 3
Milling names.

Milling name	Milling name for simplicity
U_3m_5:1_10m	U
U_75μ_5:1_10m	U_75μ
U_3m_10:1_10m	U_10:1
U_3m_5:1_5m	U_5m

Photo of U-3m initial material was taken by a digital camera (Samsung, model 'ES73'). Microstructure images of the U-3m material and U_5m milled powder were investigated by a stereo optical microscope (SOM) (Olympus, model 'SZ61') with the digital camera and also a polarizing optical microscope (POM) (Olympus, model 'BX51') with a camera (Olympus, model 'DP72') and software (Stream Basic). The sample mounting process was performed at room temperature and under air atmosphere. The U-3m material and the U_5m powder were placed on the smooth flat and transparent glass on the millimeter paper.

Nanostructure image of the U_5m powder was examined by a scanning electron microscope (SEM) (Jeol, model 'JSM-6610').

Elemental analysis of the U_5m powder was quantified by an energy dispersive X-ray spectrometer (EDS) (Oxford Inst., model 'x-act') integrated with the SEM device. Percentage values were found by mapping.

Crystalline structures of the U-3m material and the U_5m powder were analyzed by an X-ray diffractometer (XRD) (Rigaku, model 'SmartLab') with Cu K_α radiation. Based on XRD data, their average crystalline sizes (d) were calculated from the XRD line broadening by means of the Debye Scherrer's formula [24,25], which is the basic and practical formula:

$$\beta cos\theta = 0.9\lambda/d \quad (1)$$

where, β is the full width at half maximum intensity, θ is the diffraction Bragg angle, and λ is the wavelength of the X-ray (1.541 Å).

3. Results and discussion

3.1. Particle size analysis

Fig. 1 shows change of d_{50} value of the initial materials and the milled powders by milling time. d_{50} values of the U powder were found as 444.220 μm; 14.331 μm; 63.836 μm; 67.631 μm; 22.528 μm and 19.034 μm at 0 h; 0.5 h; 1 h; 2 h; 4 h and 8 h, respectively (see Table 2). According to these data, the powder particle size decreases by ~31 times in the first 0.5 h, then increases by ~4.7 times until the 2 h, and later decreases by ~3.6 times (see inset of Fig. 1). This behavior can be attributed to cold welding mechanism [26]. In other words, since powders are exposed to heavy plastic deformation during the milling process, powder particles are cold welding each other especially if they are ductile [27]. Thus, the particle size also increases. Considering these findings, it can be concluded that the levels of the milling time in milling parameters has a very large effect.

d_{50} values of the U_75μ powder were found as 11.524 μm; 21.453 μm; 18.585 μm; 15.679 μm; 13.964 μm and 18.526 μm at 0 h; 0.5 h; 1 h; 2 h; 4 h and 8 h, in turn. According to these values, there is a fluctuation in particle size during the milling process from 0 h to 8 h. The U_10:1 powder and U_5m powder behave similar to the U powder during the milling process. Considering all the data obtained, the smallest d_{50} value which is <10 μm belongs to the U_5m powder and this value was found as 8.846 μm at 0.5 h. The difference of the U_5m powder from the other powders is smaller ball size which is 5 mm instead of 10 mm. The relationship between ball size/diameter(d) and the number of contact point (n) between the balls is: $n \propto d^{-3}$. Based on this relationship, it is possible to state that the value of n is exponentially increased as the value of d is decreased. In this way, since milling efficiently depending on n value is heightened, the particle size is decreased [28]. According to the results obtained, it can be deduced that the ball size in reduction of particle size is better than the initial powder size, the BPR and the milling time.

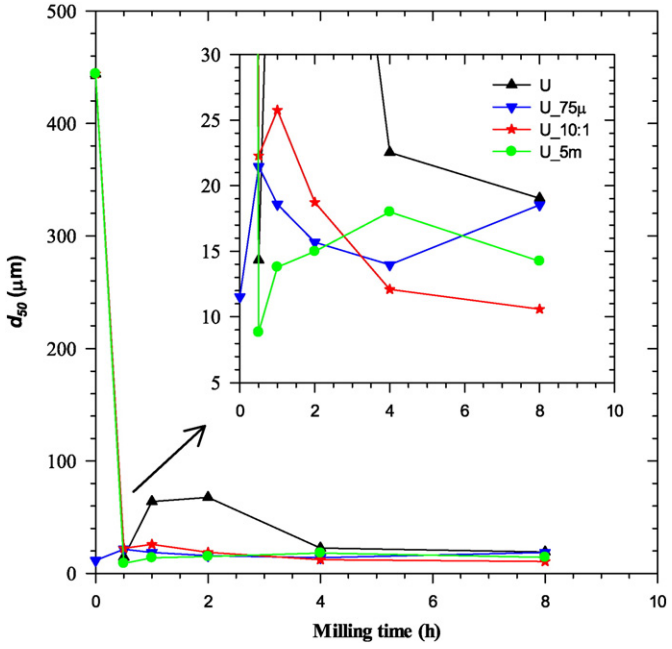

Fig. 1. The change of d_{50} value by the milling time. The inner shape is magnification for $<d_{50} = 30$ μm.

In the literature, although there are some studies on micron size of the ceramic ulexite material [2,29], no study has been conducted yet about nano size of the material.

The change of d_{10} value of the initial materials and the milled powders by milling time is given in Fig. 2. The behavior of the U powder, the U_75μ powder and the U_10:1 powder depending on the milling time is similar to the behavior at the d_{50} value. Although the change of the U_5m powder depending on the milling time is almost same between 0 h and 4 h, it is different between 4 h and 8 h. In addition, the smallest value of d_{10} is 790 nm for the U_5m powder at 0.5 h. More precisely, this value is below 1000 nm. This means that submicron level was achieved at the particle size of the ceramic ulexite material.

Fig. 3 presents the change of d_{min} value of the initial materials and the milled powders by the milling time. d_{min} value of the U powder decreases at a large amount from 0 h to 0.5 h, and then slightly decreases from 0.5 h to 1.0 h, and later slightly increases from 1 h to 8 h, respectively. d_{min} value at 0 h is 1905 nm, whereas d_{min} value at 1 h is

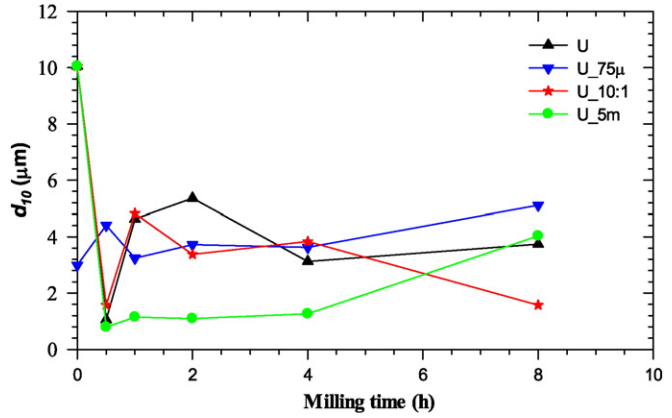

Fig. 2. The change of d_{10} value by the milling time.

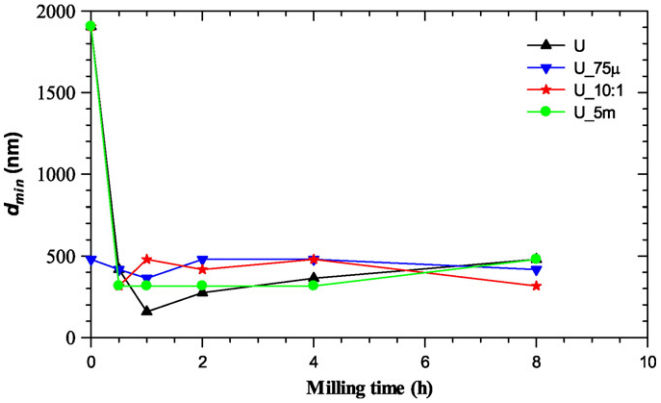

Fig. 3. The change of d_{min} value by the milling time.

158 nm which is the best value in the milled powders. Besides, optimum the milling time is 1 h for some powders, while it is 0.5 h for some others. As a result, the particle size ranges between 400 nm and 100 nm for all of them.

Change of powder mass by milling name is displayed in Fig. 4. When all powders are compared, the maximum powder loss was seen for U_75µ powder (30%), whereas the minimum powder loss was seen for U_5m powder (11%). There are multiple causes of powder loss. The most important cause is powders accumulating on the bottom of the vial over time and consequently a layer is created by hardening. This is not a desired situation in terms of application and hence the importance of milling parameters arises here. In the light of these findings, the ball size gives better results compared to others. It was thought that when the ball size becomes smaller, the space rate in milling vial becomes larger, and therefore the mobility of ball increases. In this way, the cold welding between particles decreases. Since agglomeration of the particles is avoided, the powder loss reduces and the powder yield improves simultaneously.

3.2. Morphology analysis

Fig. 5 (a) shows the photo of the U-3m initial material on the millimeter paper. Although the particle size in this material is in small amounts between 10 mm and 3 mm, it is in large amounts below 3000 µm. This means likely that the particle size is not homogeneously distributed.

A SOM image of the U-3m material, which was taken some from the material shown in Fig. 5 (a) and then placed on a glass by lightly pressing, under ×15 magnification is illustrated in Fig. 5 (b). This material

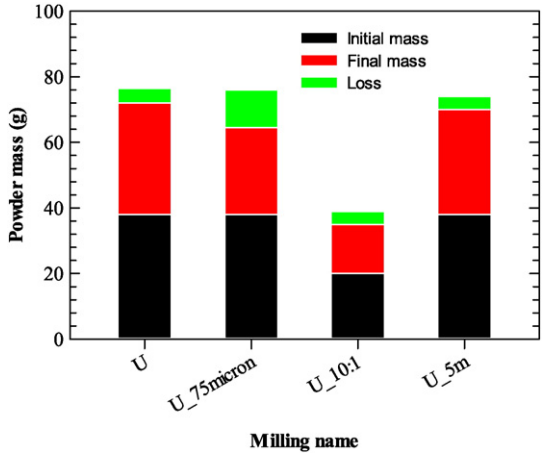

Fig. 4. The change of powder mass by the milling name.

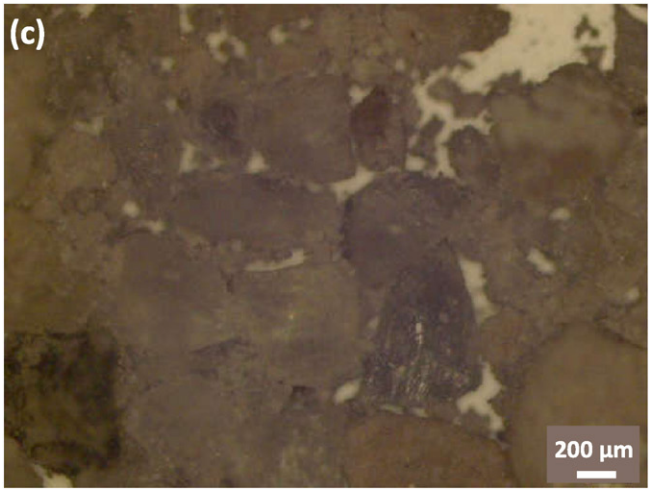

Fig. 5. Images of U-3m initial material: (a) normal (b) ×15 SOM (c) ×40 POM. Scaling was done by millimeter paper for (a) and (b).

contains various colors such as white, black, burgundy and earth color. Also, it has transparent and opaque properties. Such colors probably originate from raw material. It is known that ulexite deposits consist of some other compounds such as calcite, clay minerals, quartz, celestite, arsenic as well as pure ulexite compound [30,31]. These findings were confirmed by measurement of the oxide compound performed for this study. As it can be seen from Table 1, the presence of compounds such as SiO_2 and SO_4 as well as Na_2O, CaO and B_2O_3 oxide compounds of pure ulexite was determined in the structure of the U-3m material. In addition, the weight percent of the B_2O_3, which is precious in the

structure of the U-3m material, was found as 25.50 ± 1.50, which is the highest value in the structure.

A POM image, which was taken from the image illustrated in Fig. 5 (b), is given in Fig. 5 (c) under ×40 magnification. The particles in the U-3m material don't have smooth geometric shapes, they have sharp edges and the average size of particles is between 1000 μm and ~500 μm. The average size of particles obtained from here is approximately same as the particle size measured by the laser size analyzer (d_{50} = 444.220 μm and d_{90} = 816.708 μm, seen from Table 2).

Fig. 6 shows the POM image of U_5m milled powder at 0.5 h under ×100 magnification. The color of this powder turns into a single color (light grey) and particle size is around <100 μm. It was concluded that when the particle size of the powder is lowered, the color of powder gets lighter and aggregation increases.

Fig. 7 (a) and (b) indicate SEM images of the U_5m powder at 0.5 h under both ×500 and ×15000 magnifications, respectively. The particles of the U_5m powder seen under ×500 magnification are agglomerated. They have more smooth geometric shapes and their edges get lose mostly their sharpness in comparison with the particles of the U-3m material. Besides, the particle size of the U_5m powder ranges between ~25 μm and <1 μm. Thus, it was understood that the distribution of particle size of the U_5m powder is more uniform than that of the U-3m material. These results are in agreement with similar studies, which more homogeneous particle morphology was obtained by using the mechanical milling process [32,33]. Furthermore, these results are in agreement with the measurement results of laser size analyzer given in Figs. 1, 2 and 3, in turn.

Based on the image of the U_5m powder under ×15000 magnification, it may be said that the each particle consists of grains that are <200 nm in size. This is probably a result of the plastic deformation caused by mechanical force applied on the powder by balls during the milling process. This finding may be ascribed that the strain of average atomic level enlarges owing to the increased dislocation density with continuation of the milling process and therefore the crystal at a specific dislocation density including heavily forced regions is divided into subgrains separated by low-angle grain boundaries [27].

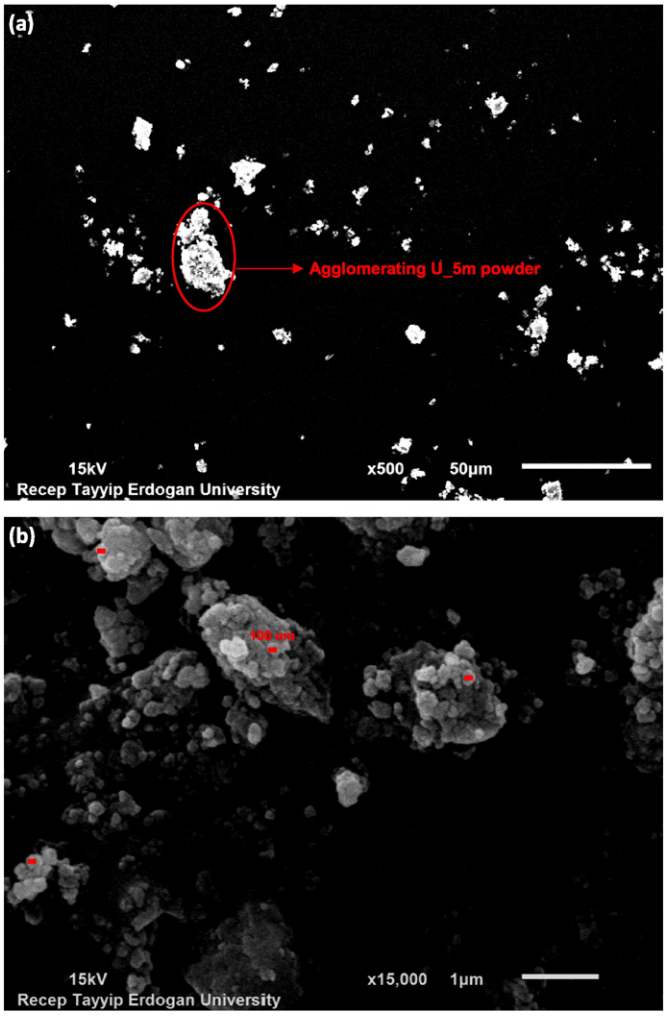

Fig. 7. The SEM images of the U_5m powder at 0.5 h: (a) under ×500 and (b) ×15000 magnification.

3.3. Elemental analysis

Fig. 8 (a) and (b) present images of the EDS region mapping for the U_5m powder at 0.5 h. The color distribution of the images was observed to be mostly same. This implies that there is a homogeneous element distribution in this structure. Fig. 8 (c) shows the spectrum of this region. Some element peaks such as Ca, O and Si were detected with the highest intensity in addition to some other element peaks such as Mg, Sr, B, Na, Al, Fe and S. The numerical values (percentages) of these elements are given in Table 4. The percentages are close to those detected in the oxide compound analysis except for boron and oxygen (see Table 1). Since the atomic number of boron (AN: 5) and oxygen (AN: 8) is smaller than 11, it is difficult to detect them. Even if they can be detected, the error margin is very large [34,35]. Besides, considering the chemical formula of ulexite compound ($Na_2O{\cdot}2CaO{\cdot}5B_2O_3{\cdot}16H_2O$), these elements indicated that there are some other compounds as well as the pure ulexite compound in the composition. These results mostly explain the different colors observed in the SOM image.

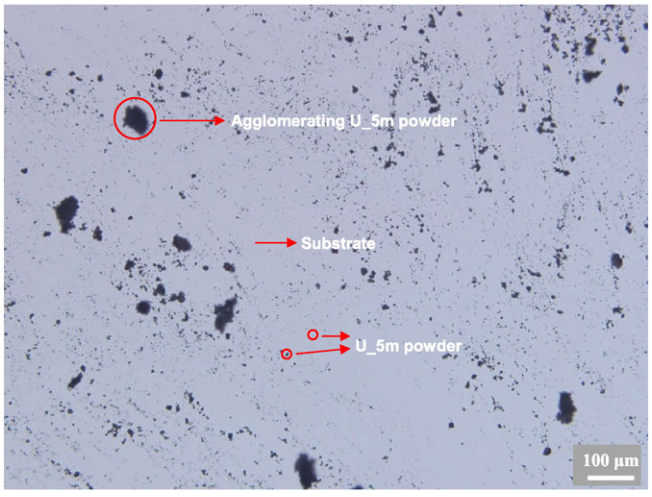

Fig. 6. The POM image of the U_5m powder at 0.5 h under ×100 magnification. Black color shows the U_5m powder and grey color shows the substrate.

3.4. Crystalline structure analysis

Fig. 9 shows the diffraction patterns of the U_5m powder for various milling time. It was determined that the structure of the U-3m material (0 h) is crystal and dominant three peaks are I = 830 (cps) for 2θ = 29.48°; I = 715 (cps) for 2θ = 13.64° and I = 384 (cps) for 2θ = 28.50°, respectively. According to the Search/Match analysis (PDXL software) of peaks of U_5m powder, it is found to be mostly coinciding with pure compound of ulexite with the chemical formula $NaCaB_5O_6(OH)_6(H_2O)_5$ and PDF Card No: 04-011-6747. Other peaks are caused by impurity compounds/elements. This finding confirms the results of elemental analysis.

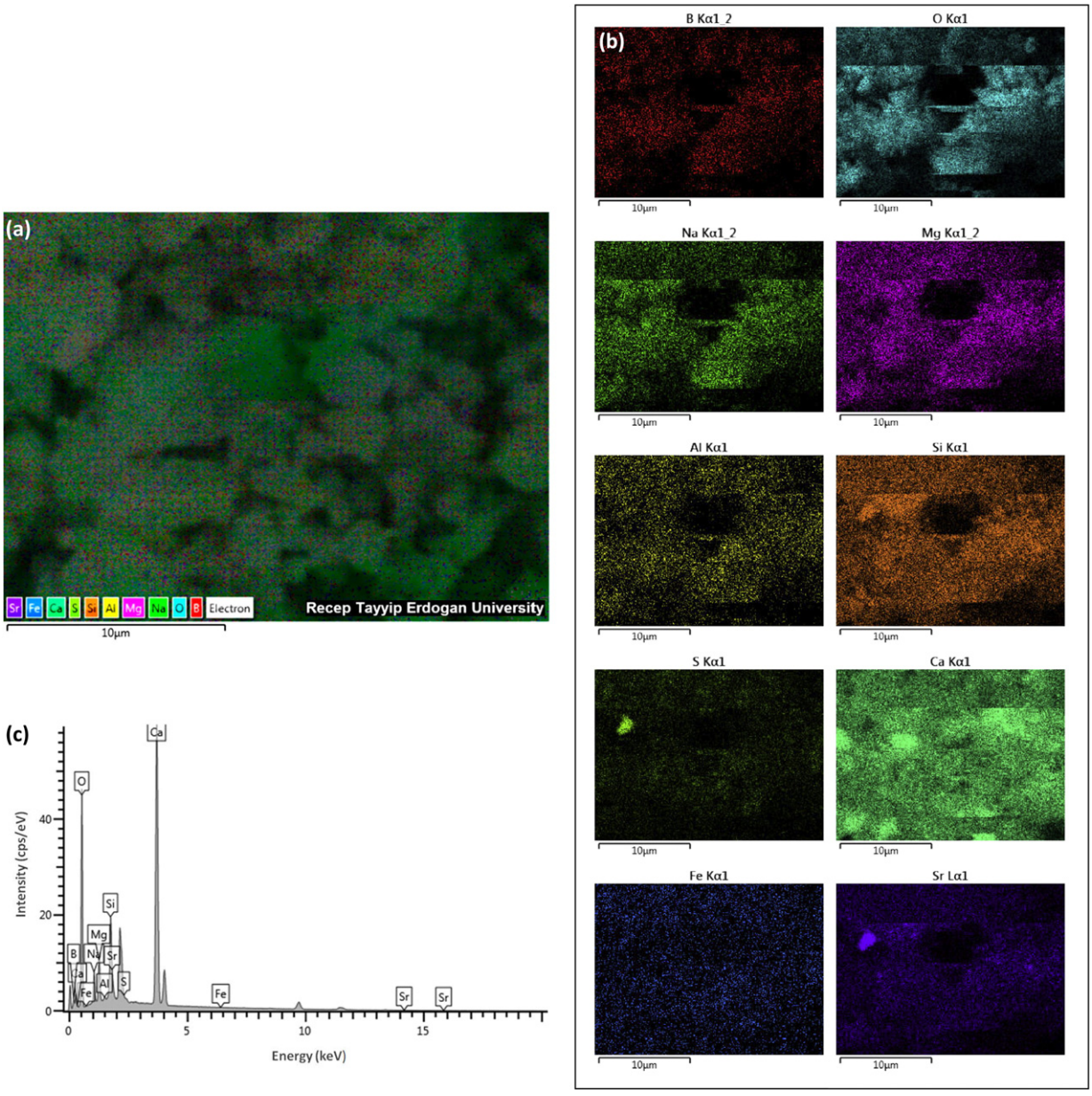

Fig. 8. EDS mapping for the U_5m powder at 0.5 h: (a) the image of the region for all elements (b) the image of the region for a single element (c) the spectrum of the region.

Several important results were obtained by milling the U_5m powder for 0.5 h, 1 h, 2 h, 4 h, and 8 h. First, the intensity of the peaks belonging to both the pure ulexite compound and impurity is reduced gradually and the crystal structure turns into an amorphous structure after 8 h. Second, the width of the peaks gradually increases. Third, impurity peak at $2\theta = 13.73°$ get lost in a shorter time than others. In the light of all these findings, it was concluded that particles are deformed as a result of the mechanical milling process and simultaneously their crystal structures are deformed.

Table 4
EDS mapping for elemental analysis of the U_5m powder at 0.5 h.

Element	Compound weight (%)	Compound error (%)
O	62.2	0.8
Ca	20.5	0.3
B	6.6	1.2
Si	3.4	0.1
Na	2.8	0.1
Mg	2.6	0.0
Sr	1.2	0.1
Al	0.3	0.0
S	0.3	0.0
Fe	0.1	0.0
Total	100.0	

The crystalline size of the U_5m powder as the function of the milling time is given in Fig. 10. The crystalline sizes were found as 59.8 nm, 36.2 nm, 23.2 nm, 18.7 nm, 15.5 nm and null nm for 0 h, 0.5 h, 1 h, 2 h, 4 hand 8 h milling times, in turn. Considering all these data, it was determined that the crystalline size decreases exponentially with increasing milling time and is also reduced by 39% after 0.5 h of milling and 74% after 4 h of milling.

Although there are several studies about crystal structure analysis of the ceramic ulexite material in the literature [31,36], no studies have been conducted yet about that of its mechanical milling process or nano size.

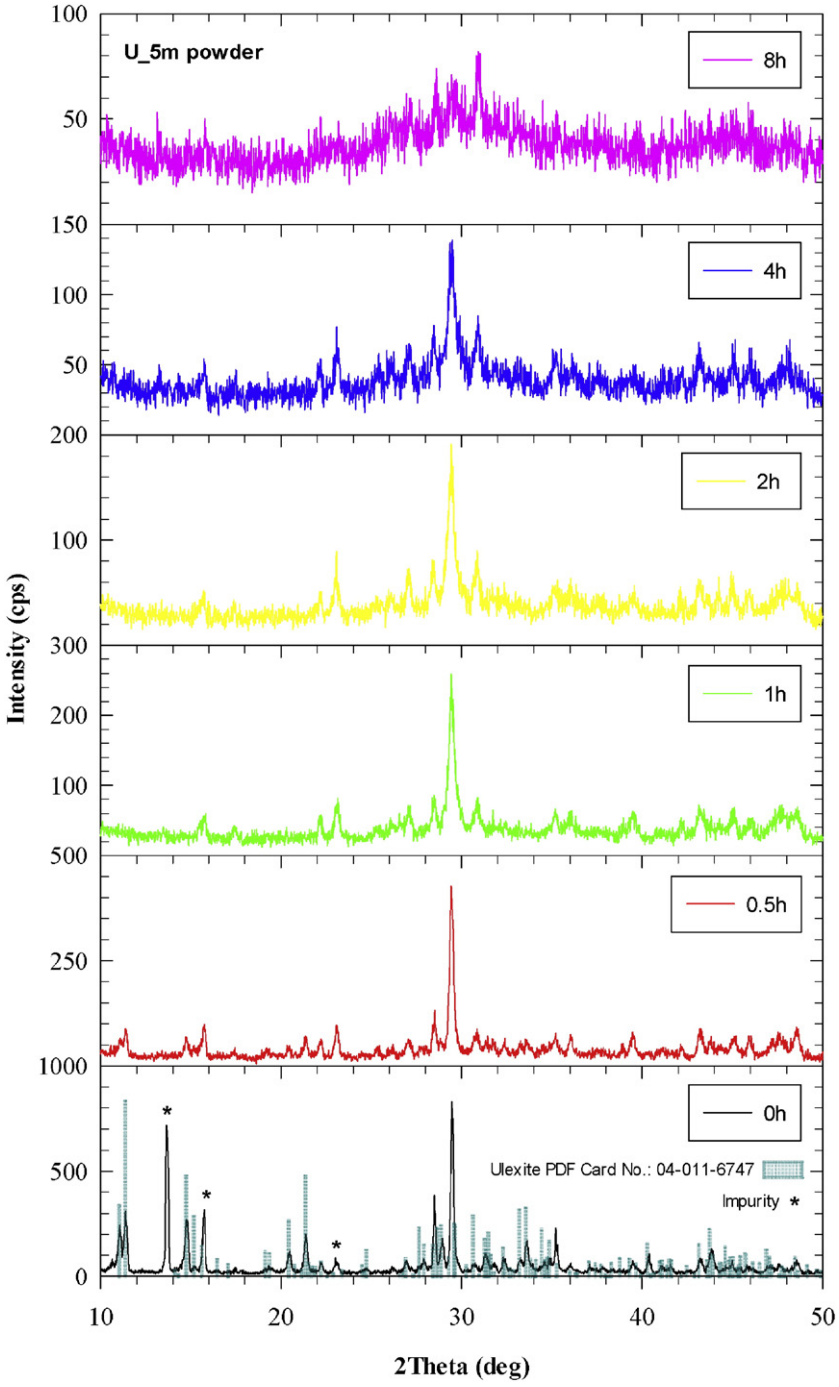

Fig. 9. Diffraction patterns of the U_5m powder by the milling time.

4. Conclusion

Some important findings which may be useful for next researches in this field can be drawn below.

✓ Among milled ulexite powders, the smallest d_{50} value was found as 8.846 μm for the U_5m powder. The U-3m initial material is reduced to this value after 0.5 h of milling from 444.220 μm (unmilled, 0 h). This result showed that in the milling parameters, the ball size gives better results compared to the initial powder size, the BPR and the milling time.

✓ The smallest d_{10} value was determined as 790 nm for the U_5m powder at 0.5 h. This result indicated that the levels of the milling time have serious significance.

✓ The value of d_{min} ranges between 400 nm and 100 nm for the milled powders.

✓ It was decided that the U-3m material contains different colors and this is caused by that the ulexite is not a pure compound. This is confirmed by not only oxide compound analysis but also EDS analysis.

✓ Powder morphology of the U_5m powder is improved after the milling process.

✓ The crystal structure of the U_5m powder turns into amorphous after about 8 h of milling.

✓ The crystalline size of the U_5m powder decreases exponentially with the milling time and is reduced to 15.5 nm after 4 h.

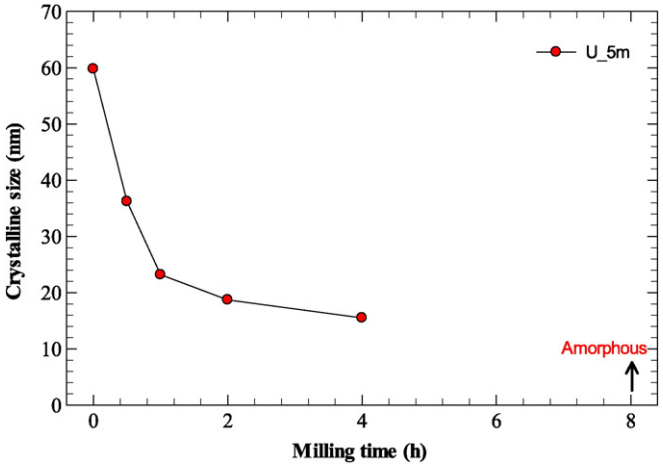

Fig. 10. The crystalline size of the U_5m powder as a function of the milling time.

Acknowledgement

The author would like to thank the Scientific Research Projects Unit of Recep Tayyip Erdogan University (project contract no: 2014.109.03.01) for giving financial support; the Eti Maden for providing ulexite materials; Asst. Prof. T. Kutuk-Sert, project manager, for allowing for detailed research; Assoc. Prof. A. Canakci for measuring the laser size analyzer and Asst. Prof. Y. Demir for using optical microscope.

References

[1] Eti Mine, Annual Raport, Ankara, 2013 35.
[2] H. Ipek, H. Sahan, Effect of heat treatment on breakage rate function of ulexite, Physicochem. Probl. Miner.Process. 49 (2013) 651–658.
[3] N. Demirkiran, N. Bayrakci, C. Asin, Dissolution of thermally dehydrated ulexite in ammonium acetate solutions, Trans. Nonferrous Metals Soc. China 23 (2013) 1797–1803.
[4] H. Sert, H. Yıldıran, D. Toscalı, An investigation on the production of sodium metaborate dihydrate from ulexite by using trona and lime, Int. J. Hydrog. Energy 37 (2012) 5833–5839.
[5] M. Vignolo, G. Bovone, D. Matera, D. Nardelli, C. Bernini, A.S. Siri, Nano-sized boron synthesis process towards the large scale production, Chem. Eng. J. 256 (2014) 32–38.
[6] F. Demir, A. Un, Radiation transmission of colemanite, tincalconite and ulexite for 6 and 18 MV X-rays by using linear accelerator, Appl. Radiat. Isot. 72 (2013) 1–5.
[7] S. Guo, C. Hu, Y. Kagawa, D. Butt, Mechanochemical processing of nanocrystalline zirconium diboride powder, J. Am. Ceram. Soc. 94 (2011) 3643–3647.
[8] U.K. Sevim, Y. Tümen, Strength and fresh properties of borogypsum concrete, Constr. Build. Mater. 48 (2013) 342–347.
[9] T. Kutuk-Sert, S. Kutuk, Physical and Marshall properties of borogypsum used as filler aggregate in asphalt concrete, J. Mater. Civ. Eng. 25 (2013) 266–273.
[10] C.B. Emrullahoglu Abi, Effect of borogypsum on brick properties, Constr. Build. Mater. 59 (2014) 195–203.
[11] M. Alizadeh, F. Sharifianjazi, E. Haghshenasjazi, M. Aghakhani, L. Rajabi, Production of nanosized boron oxide powder by high-energy ball milling, Synth. React. Inorg. Met.-Org. Chem. 45 (2015) 11–14.
[12] A. Canakci, H. Cuvalci, T. Varol, E.D. Yalcın, S. Ozkaya, F. Erdemir, Synthesis of novel CuSn10-graphite nanocomposite powders by mechanical alloying, IET Micro Nano Lett. 9 (2014) 109–112.
[13] F.L. Zhang, M. Zhu, C.Y. Wang, Parameters optimization in the planetary ball milling of nanostructured tungsten carbide/cobalt powder, Int. J. Refract. Met. Hard Mater. 26 (2008) 329–333.
[14] M. Abdellahi, H. Bahmanpour, M. Bahmanpour, The best conditions for minimizing the synthesis time of nanocomposites during high energy ball milling: modeling and optimizing, Ceram. Int. 40 (2014) 9675–9692.
[15] Y. Li, Y. Wang, Q. Lv, Z. Qin, X. Liu, Synthesis of uniform plate-like boron nitride nanoparticles from boron oxide by ball milling and annealing process, Mater. Lett. 108 (2013) 96–102.
[16] J. Jung, J. Kim, Y.R. Uhm, J.-K. Jeon, S. Lee, H.M. Lee, C.K. Rhee, Preparations and thermal properties of micro- and nano-BN dispersed HDPE composites, Thermochim. Acta 499 (2010) 8–14.
[17] X. Xu, J.H. Kim, W.K. Yeoh, Y. Zhang, S.X. Dou, Improved Jc of MgB2 superconductor by ball milling using different media, Supercond. Sci. Technol. 19 (2006) L47–L50.
[18] H.J. Jung, Y. Sohn, H.G. Sung, H.S. Hyun, W.G. Shin, Physicochemical properties of ball milled boron particles: dry vs. wet ball milling process, Powder Technol. 269 (2015) 548–553.
[19] P. Zhang, D. Jia, Z. Yang, X. Duan, Y. Zhou, Physical and surface characteristics of the mechanically alloyed SiBCN powder, Ceram. Int. 38 (2012) 6399–6404.
[20] P. Zhang, D. Jia, Z. Yang, X. Duan, Y. Zhou, Influence of ball milling parameters on the structure of the mechanically alloyed SiBCN powder, Ceram. Int. 39 (2013) 1963–1969.
[21] Eti Mine, Product Catalogue of Eti Mine: Bigadic Ulexite, 2014 2.
[22] Eti Mine, Product Catalogue of Eti Mine: Milled Ulexite, 2014 3.
[23] S. Bolat, S. Kutuk, Fabrication of the new $Y_3Ba_5Cu_8O_y$ superconductor using melt-powder-melt-growth method and comparison with $YBa_2Cu_3O_{7-x}$, J. Supercond. Nov. Magn. 25 (2012) 731–738.
[24] S.N. Alam, Synthesis and characterization of W–Cu nanocomposites developed by mechanical alloying, Mater. Sci. Eng. A 433 (2006) 161–168.
[25] C. Kursun, M. Gogebakan, Characterization of nanostructured Mg–Cu–Ni powders prepared by mechanical alloying, J. Alloys Compd. 619 (2015) 138–144.
[26] S. Sivasankaran, K. Sivaprasad, R. Narayanasamy, V.K. Iyer, An investigation on flowability and compressibility of AA 6061100 – x-x wt.% TiO2 micro and nanocomposite powder prepared by blending and mechanical alloying, Powder Technol. 201 (2010) 70–82.
[27] C. Suryanarayana, Mechanical alloying and milling, Prog. Mater. Sci. 46 (2001) 1–184.
[28] H. Shin, S. Lee, H. Suk Jung, J.-B. Kim, Effect of ball size and powder loading on the milling efficiency of a laboratory-scale wet ball mill, Ceram. Int. 39 (2013) 8963–8968.
[29] S. Sener, G. Ozbayoglu, S. Demirci, Changes in the structure of ulexite on heating, Thermochim. Acta 362 (2000) 107–112.
[30] Ö. Yildiz, The effect of heat treatment on colemanite processing: a ceramics application, Powder Technol. 142 (2004) 7–12.
[31] M.F. Eskibalci, S.G. Ozkan, An investigation of effect of microwave energy on electrostatic separation of colemanite and ulexite, Miner. Eng. 31 (2012) 90–97.
[32] T. Varol, A. Canakci, Effect of particle size and ratio of B4C reinforcement on properties and morphology of nanocrystalline Al2024-B4C composite powders, Powder Technol. 246 (2013) 462–472.
[33] T. Kutuk-Sert, Stability analyses of submicron-boron mineral prepared by mechanical milling process in concrete roads, Constr. Build. Mater. 121 (2016) 255–264.
[34] S.K. Mishra, S. Das, L.C. Pathak, Defect structures in zirconium diboride powder prepared by self-propagating high-temperature synthesis, Mater. Sci. Eng. A 364 (2004) 249–255.
[35] S. Kutuk, S. Bolat, C. Terzioglu, S.P. Altintas, An investigation of magnetoresistivity properties of an $Y_3Ba_5Cu_8O_y$ bulk superconductor, J. Alloys Compd. 650 (2015) 159–164.
[36] S.U. Bayca, F. Kocan, Y. Abali, Investigation of leaching kinetics of ulexite waste in oxalic acid solutions, Chem. Biochem. Eng. Q. 28 (2014) 273–280.